Land Remote Sensing
Lab 06: Volcano Monitoring

Assigned: November 13, 2017
Due: November 20, 2017

In this lab, you will generate several figures. Please sensibly name these figures, save them as .png or similar, collect them into a single .zip file named `xxxxxx_lab06.zip` where xxxxxx is your last name, and e-mail them to `gleggers@gatech.edu` with the subject line of "`[EAS 8803] Lab 06 Products.`"

Any files you need are at: http://wray.eas.gatech.edu/remotesensing2017/RS_lab06_files.zip.

Volcanoes are breaches in Earth's surface that spew forth hot lava, ash, and gases from magma chambers deep below. As one of the most raw displays of Earth's power, eruptions can be incredibly deadly, especially when they initiate secondary events like lahars and pyroclastic density currents. However, even eruptions in remote, sparsely populated areas like the Aleutian Islands are problematic as their hot ash plumes can wreak havoc on international flight paths. Still, no orbital infrastructure is dedicated to these phenomena, and what monitoring exists takes advantage of preexisting spacecraft and incidents.

In prior labs, we have dealt independently with various remote sensing methods, but these methods are often used in conjunction to study the same problem from different angles. In this lab, you will explore how visible, thermal, and UV spectroscopy can all be applied to the problem of volcano monitoring. In the following sections, each method is paired with a case study eruption that exhibits the method. Eruption details are given in brief, but for more information check the Smithsonian's Global Volcanism Program at https://volcano.si.edu.

1 Visual Change with Landsat-8

Volcanic eruptions can cause visible changes to Earth's surface. Examples include blanketing ash from a plume, lava flows, or even collapse of the volcanic edifice. The Landsat program is the longest-running enterprise to monitor these and other land surface changes. The program's most recent iteration is Landsat-8, which was launched on February 11, 2013. Its OLI (Operational Land Imager) sensor collects data in the visible to shortwave infrared wavelengths at a resolution of 30 meters with a repeat cycle of 16 days.

Holuhraun (64.888°N, 16.711°W) is an Icelandic lava field that resulted from immense volcanic activity on the Bárðarbunga and Askja fissure systems. Precrursed by seismic activity, on August 29, 2014, an old 600 m fissure began erupting, bollowed by a 1.5 km long fissure on August 31. Volcanic activity peaked in late January 2015 and gradually decreased until it ceased on February 27, almost six months later.

Landsat imagery can be accessed from the EarthExplorer portal at https://earthexplorer.usgs.gov/, but for this lab, use the scenes in the `holuhraun` subdirectory. Two Landsat-8 images over Holuhraun are provided: one from July 24, 2013 before the most recent eruption (`ls8_218014_20130724.tif`) and one from September 25, 2015 after the most recent eruption (`ls8_217015_20150925.tif`).

1. What changes do you observe at Holuhraun from pre- to post-eruption?
2. Estimate the area of the lava field from the 2014-2015 eruption.

2 Thermal Anomaly with MODIS

Volcanoes erupt materials at elevated temperatures. Rhyolitic lavas are often in the range of 650 to 800°C while basaltic lavas can be up to 1000-1200°C. Surface temperatures case even rise prior to eruptions as underlying magma ascends. Routine thermal monitoring is often done with the twin MODIS (MODerate-resolution Imaging Spectroradiometer) sensors aboard the Terra and Aqua satellites, which have 36 bands between 0.405 and 14.385 µm with spatial resolutions of 250 m (bands 1–2), 500 m (bands 3–7), and 1000 m (bands 8-36) at nadir. Between the two sensors, most regions can be revisited four times a day (morning, afternoon, late evening, and night). Using MODIS thermal data processed via the MODVOLC algorithm, the Hawai'i Institute of Geophysics monitors thermal anomalies in near real-time by identifying pixels with elevated temperatures (from lava flows, wildfires, etc.) as inferred from a spike in spectral radiance at 3.959 µm (bands 21 and 22). The MODVOLC interface and documentation can be found at http://modis.higp.hawaii.edu/.

Kīlauea (19.406°N, 155.283°W) is a basaltic shield volcano on the island of Hawai'i—the second youngest product of the Hawaiian hotspot. The volcano has been continuously erupting since January 3, 1983. Since 2015, surficial activity has consisted off lowering, raising, and occasional overflows of the Halemaʻumaʻu and Puʻu ʻŌʻō crater lava lakes and breakouts along various lava flows, especially the northeast trending flow.

From the MODVOLC website, navigate to Kīlauea and view the aggregate thermal anomalies for December 10 to December 16, 2016 for both daytime and nighttime on both Terra and Aqua.

3. How many distinct distributions of thermal anomalies are present? What physical features or activities explain the locations and shapes of those distribution?

4. Choose "View Alert Data" and find the thermal alert from December 12 at (19.401756°N, 155.282166°W). Using the 3.959 µm spectral radiance, calculate a brightness temperature. Is this temperature typical for erupted lavas? If not, what might be causing the difference?

3 Plume Tracking with OMPS

Volcanic eruptions are driven by exsolving magmatic gases, typically H_2O, CO_2, and SO_2, and after exiting the vent these gases may drift with hot and dangerous airborne ash as a volcanic plume. SO_2 is used to monitor these plumes because the concentration of SO_2 output by volcanoes greatly exceeds the gas's background atmospheric levels relative to the other volcanic gases. With 10 distinctive spectral features in the ultraviolet, SO_2 is easily detected by the Suomi NPP satellite's OMPS (Ozone Mapper Profiler Suite), a hyperspectral UV sensor with a 50 km resolution at nadir and daily revisit time. Using OMPS (and OMI, another UV ozone sensor) data and a linear fit algorithm, NASA's Atmospheric Chemistry and Dynamics Laboratory monitors volcanic plumes and other SO_2 emissions in near real time. The Global Sulfur Dioxide Monitoring data and documentation can be found at http://so2.gsfc.nasa.gov/.

Pavlof (55.418°N, 161.893°W) is a snow- and ice-covered stratovolcano with a summit elevation of 2518 m located on the southwestern end of the Alaska Peninsula. On March 27, 2016, an increase in seismicity was reported at Pavlof as well as an ash plume rising to 6.1 km above sea level. That night, lava fountaining was observed. On the morning of March 28, the ash plume had reached 11 km in altitude and drifted more than 650 km. By March 29, eruptive activity had largely subsided.

From the Global Sulfur Dioxide Monitoring home page, navigate to the Alaska region and then to OMPS data for March 2016. Find the plume associated with the Pavlof eruption.

5. From what direction is the prevailing wind, and how quickly did the coherent SO_2 plume form and disperse? What populated areas may have affected by the plume?

6. Calculate the column mass of SO_2 for the pixel with the highest SO_2 concentration. A Dobson Unit (DU) is defined as 2.69×10^{16} molecules/cm^2, and assume the pixel is near nadir.

4 Bogoslof: An Integrative Example

All of the orbiters discussed were designed for primary objectives other than volcano monitoring. Their data may have later been co-opted for that purpose, but consequently the sensors were not optimized for the unique challenges of observing volcanic systems. The case studies shown previously were "quality" examples of the phenomena they were to demonstrate, but they do not represent a "typical" volcanic event.

Bogoslof (53.932°N, 168.037°W) is the emergent summit of a submarine volcano that rises 1500 m above the Bering Sea floor north of the Aleutian island arc. It has exhibited several periods of activity over the last 100+ years, periodically building and destroying subaerial lava domes. The current eruption at Bogoslof began in mid-December and is ongoing with frequent seismic activity, explosions, and small ash plumes.

7. On January 18, 2017, a large event was observed by several orbiting sensors and is the focus for this section. For this "more typical" volcanic event, do the following:

(a) The `bogoslof` subdirectory contains two Landsat-8 images: one from February 24, 2015 before the current eruptive sequence (`ls8_077023_20150224.tif`) and one from January 28, 2017 after the January 18th event (`ls8_077023_20170128.tif`). Describe the changes to Bogoslof island, and estimate the change in surface area of the island.

(b) Navigate to Bogoslof from the MODVOLC website. Calculate a brightness temperature using the 3.959 µm spectral radiance for the brighter thermal anomaly.

(c) Navigate to the Aleutian Islands region OMPS data from the Global Sulfur Dioxide Monitoring home page. Is an SO_2 plume present? If so, in what direction is it traveling and calculate the column mass of SO_2 for the pixel with the highest concentration. Assume the pixel is near nadir.

8. Compare and contrast your calculations for the "typical" case of Bogoslof versus the more "ideal" cases of Holuhraun, Kīlauea, and Pavlof for each remote sensing method. Taking into account spatial, temporal, and spectral resolution, what is the utility of each orbiting sensor to regular and routine monitoring of volcanic activity?

5 Active Volcanism on Venus?

Venus' surface betrays its volcanic past, but it is unknown whether its volcanism is ongoing. Orbiting the planet from April 2006 to December 2014, the European Space Agency's Venus Express provided several lines of evidence supporting recent volcanic activity. Using the VIRTIS (Visible and Infrared Thermal Imaging Spectrometer) instrument, *Smrekar et al.* (2010) studied thermal emissivity variation on lava flows at three Venusian "hotspots," identifying compositional differences interpreted to represent lack of weathering and thus a young surface. With the SPICAV (Spectroscopy for Investigation of Characteristics of the Atmosphere of Venus) UV sensor, *Marcq et al.* (2013) reported strong latitudinal and temporal variability in SO_2 column density consistent with supply variations from the lower atmosphere, which could represent occasional injections of SO_2 into the Venusian cloud tops from buoyant volcanic plumes. Finally, from VMC (Venus Monitoring Camera) data, *Shalygin et al.* (2015) identified transient thermal anomalies indicating local elevated temperatures at the young Ganiki Chasma, which is appears similar to terrestrial rift systems. These papers are provided in the `venus` subdirectory for perusal at your leisure.

9. **[BONUS]** Given recent (ESA's Venus Express) and current (JAXA's Akatsuki) orbital assets at Venus, briefly discuss our ability to adequately characterize extant volcanic activity. Think in terms of the broad eruptions styles examined in this lab: large and long-lived but infrequent eruptions like Holuhraun, small and continuous eruptions like Kīlauea, or moderate and frequent eruptions like Pavlof. Be sure to consider both the instrumentation of these orbiter and their spatial/temporal/spectral resolutions, as well as the unique geophysical and atmospheric conditions of Venus.

Appendix: Volcano Photos

A Holuhraun

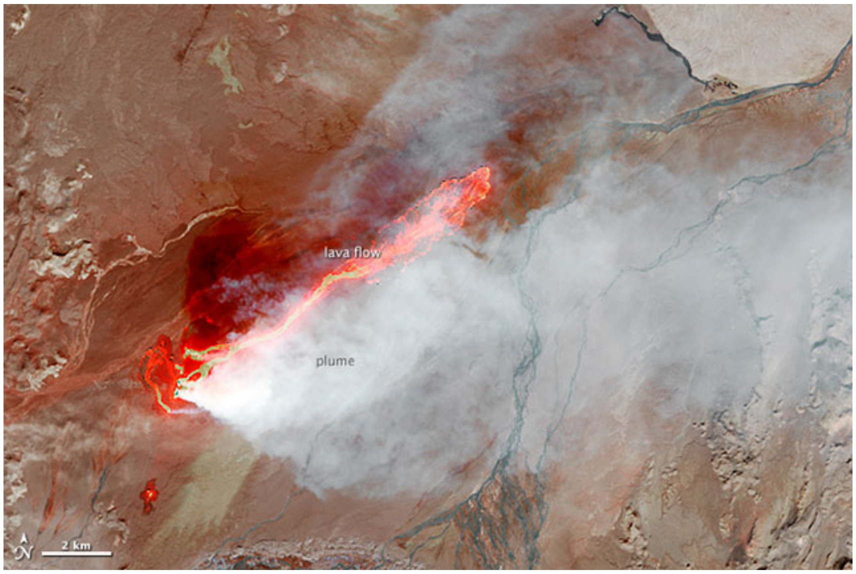

Figure 1: Landsat-8 view of lava fountaining, lava flows, and plumes emerging from Holuhraun on September 6, 2014.

Figure 2: Lava fountaining from an erupting fissure with a lava flow coming off the side.

Figure 3: Advancing lava field.

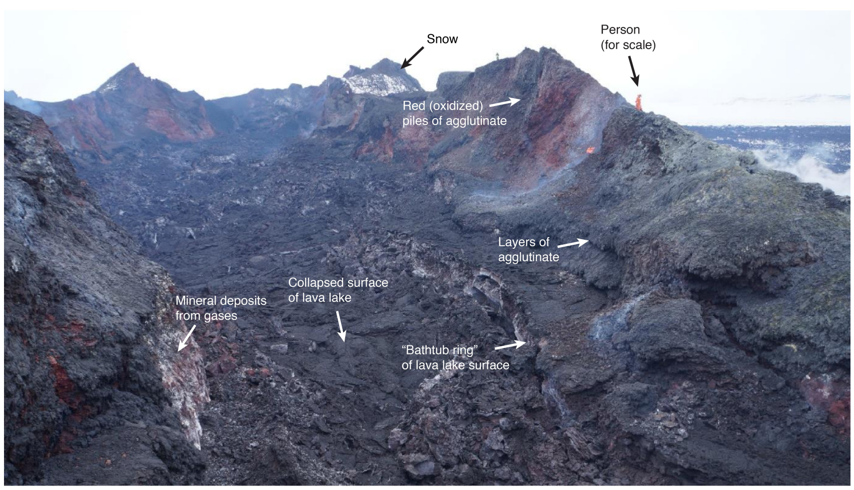

Figure 4: Annotated view inside the Holuhraun crater days after the eruption ended. A few weeks before, it was filled with an active lava lake and vent. Note the person for scale.

B Kīlauea

Figure 5: The Halema'uma'u lava lake at Kilauea on September 7, 2016 when the surface level was at the level of the old crater rim (8 m below the current rim).

Figure 6: Lava flow crossing a FEMA emergency access road. On left is the flow on July 25, 2016 about 30 minutes after it crossed. On right is on August 5 and shows flow inflation. Note the geologist for scale.

Figure 7: Small breakout from a pāhoehoe lava flow on the coastal plain of Kīlauea on September 20, 2016. Burning vegetation on the pali (cliff) from the recent flow is visible in the background.

Figure 8: Lava flowing into the sea at Kīlauea from one of the entry points along the Kamokuna ocean entry on September 11, 2016. As the lava freezes, it adds new land to the island.

C Pavlof

Figure 9: Summit crater of Pavlof Volcano on July 23, 2017.

Figure 10: Pavlof erupting and sending a plume of volcanic ash into the air on the evening of March 27, 2016.

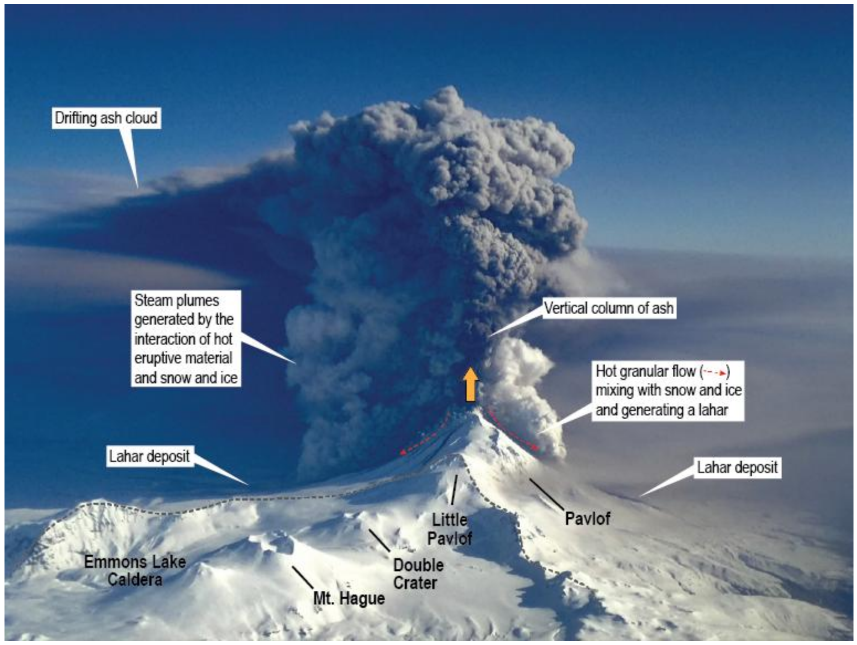

Figure 11: Pavlof continuing to erupt on March 28, 2016 with several younger post-caldera volcanoes in the foreground. Annotations show several of the processes that were occurring during the eruption.

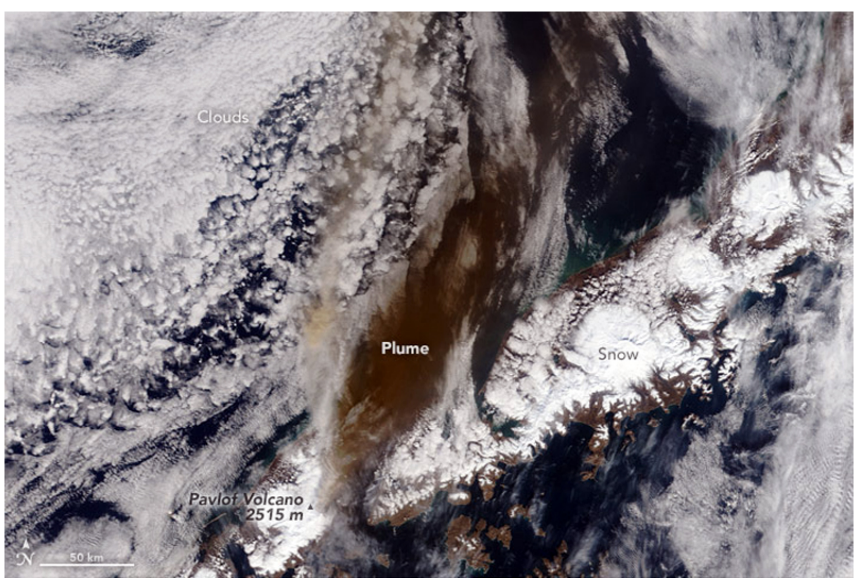

Figure 12: Image of the ash plume from Pavlof at 11:45 AKDT on March 28, 2016 captured by the MODIS instrument. The plume extends for several hundred kilometers.

D Bogoslof

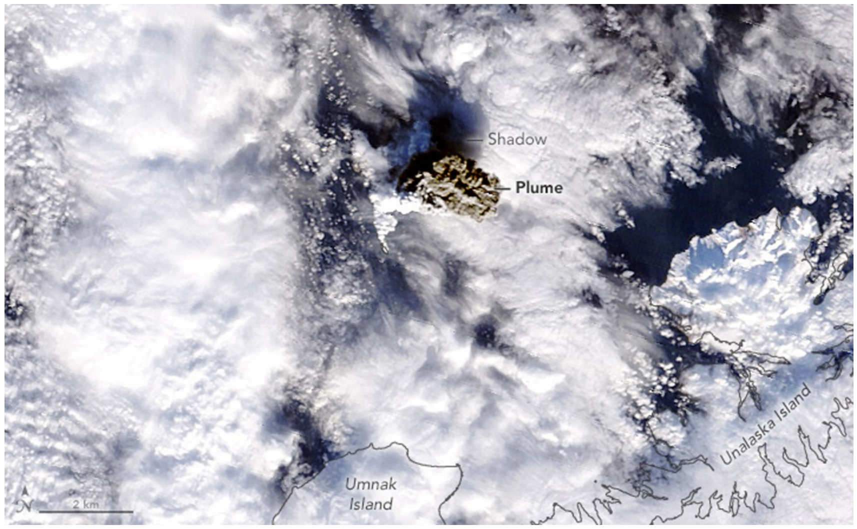

Figure 13: A large explosion on January 18, 2017 produced a dark ash cloud that rose to 9.4 km. Captured by MODIS.

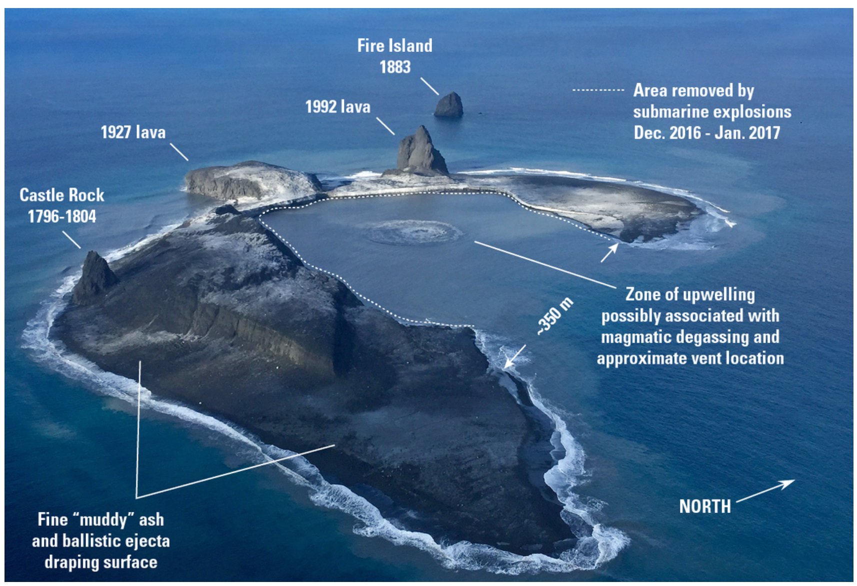

Figure 14: Annotated photograph of Bogoslof Island from January 10, 2017 showing the cumulative effects at the time of the 2016-17 eruptive activity.

Figure 15: Bogoslof Island viewed from the northwest on May 8, 2017. Fire Island is in the right foreground, and the new steaming lake, which includes the submarine vent, is behind the two dome remnants in the foreground.

Figure 16: A small portion of a northern fur seal rookery on Bogoslof Island in 2015. Northern fur seal and Steller sea lion populations congregate on the island for the pupping and breeding seasons.